Expression of n-MYC, NAMPT and SIRT1 in Basal Cell Carcinomas and their Cells of Origin

Lydia BRANDL[1], Daniela HARTMANN[2], Thomas KIRCHNER[1,3] and Antje MENSSEN[1]
[1]Institute of Pathology, [2]Department of Dermatology and Allergology, Ludwig-Maximilians University, Munich, and [3]German Consortium for Translational Cancer Research (DKTK), DKFZ, Heidelberg, DKTK Site, Munich, Germany

Deregulated Hedgehog signalling is a driver of basal cell carcinomas. One effector of the Hedgehog pathway is n-MYC. c/n-MYC proteins, NAMPT and DBC1 are linked to SIRT1 in a positive feedback loop that may contribute to tumorigenesis of basal cell carcinoma. In 5 basal cell carcinoma types immunohistochemistry revealed n-MYC, NAMPT and SIRT1 expression. DBC1 was homogenously expressed in all epithelial cells. NAMPT, SIRT1 and c-MYC were expressed in the stratum basale of human and murine skin. In hair follicles NAMPT and SIRT1 were expressed together with c-MYC and n-MYC, except for the matrix, where n-MYC was strongly positive, but c-MYC expression was absent. Therefore, a common pathway connecting n-MYC, NAMPT and SIRT1 may be active in basal cell carcinomas and in their cells of origin. This pathway may contribute to the development of basal cell carcinomas. Targeting factors in the feedback loop may offer novel therapeutic options.

SIGNIFICANCE

Basal cell carcinoma is a skin tumour with locally aggressive growth. Analysing human basal cell carcinomas, and human and murine normal skin, including hair follicles, we show that the proteins of the c-MYC-NAMPT-DBC1-SIRT1 positive feedback loop may be active in both the skin stem cell areas, which are considered the cells of origin, and in basal cell carcinomas. Therefore, the positive feedback loop may play a crucial role in the development of basal cell carcinomas. Since NAMPT and SIRT are targetable enzymes, our results may open novel avenues for therapeutic interventions in basal cell carcinomas.

The Hedgehog (Hh) pathway harbours prevalent somatic mutations and is a central driver of basal cell carcinoma (BCC) development. These mutations include loss-of-function mutations in the Hh receptor Patched 1 (*PTCH1*) gene (73%), or activating mutations in Smoothened (*SMO*) (20%)). Furthermore, BCCs typically harbour mutations in the Hippo-YAP pathway (*PTPN14* (23%), *LATS1* (16%)), and in *TP53* (61%), the hTERT promoter, and in the *DPH3-OXNAD1* bidirectional promoter (42%). Recently, additional oncogenic alterations have been uncovered that explained the heterogeneous nature of BCCs (reviewed in (1)). Hair follicle (HF) stem cells have been postulated to represent the cell of origin of BCC, since they share many characteristics with BCCs. In addition, interfollicular epidermis (IFE) progenitor cells may give rise to BCCs (2, 3).

An important downstream mediator of Hh signalling is the n-MYC proto-oncogene protein (4), which is activated by Hh-induced transcriptional and post-transcriptional mechanisms (5–7). Since the Hh and Wnt pathways are connected through cross-regulation (8), Wnt pathway

activation may also contribute to BCCs by transcriptional induction of the β-catenin/TCF4 target gene *MYCN*. We, and others, have shown that the constitutive activation of the Wnt pathway in BCCs is reflected by the accumulation, stabilization and nuclear translocation of β-catenin, and nuclear LEF1 expression (9, 10).

n-MYC and c-MYC belong to the MYC family of transcription factors. They have an homologous amino acid sequence in functionally relevant domains and they share the same canonical E-box DNA motives, overlapping target genes and many functions (11, 12). MYC proteins regulate processes associated with proliferation, such as the regulation of cell cycle entry, DNA replication, protein synthesis, block of differentiation and metabolism. Deregulation of MYC proteins is a common feature of most cancers (reviewed in (13)). We, and others have shown that the NAD⁺-dependent deacetylase silent information regulator 1 (SIRT1) is downstream of c-MYC, and of n-MYC (14, 15). SIRT1 is involved in the regulation of transcription, apoptosis, DNA damage repair, metabolism, and triggers resistance to cellular stressors, such as DNA damage, oxidative stress and fasting (16). While various pro-apoptotic factors, including p53, are negatively regulated by SIRT1, SIRT1 is linked to c-MYC and n-MYC through a positive feedback loop. The SIRT1 protein is overexpressed in the majority of solid and haematopoietic malignancies. It acts as a survival factor for cancer cells and cancer stem cells and contributes to tumour cell drug resistance. An important function of SIRT1 in cancer may be to counteract apoptosis, senescence and cell cycle arrest, thus supporting survival and permanent tumour cell proliferation (reviewed in (16–18)). We identified the NAD⁺ salvage pathway enzyme nicotinamide phosphori-

bosyltransferase (NAMPT) as a direct c-MYC target gene that leads to the production of the SIRT1 cofactor NAD$^+$ and SIRT1 activation (15).

Furthermore, we have established that the c-MYC-NAMPT-DBC1-SIRT1 positive feedback loop may play a role in classical and serrated route colorectal cancer (15, 19). Studies in various animal models have confirmed that the c-MYC-SIRT1 regulatory circuitry contributes to tumorigenesis. To identify disease-relevant pathways and novel drug targets for BCC, we determined the expression of c-MYC and n-MYC, NAMPT, SIRT1, and the negative regulator of SIRT1, the deleted in breast cancer 1 (DBC1) protein, also called CCAR2 (Cell Cycle And Apoptosis Regulator 2) in 65 BCCs, in normal skin and in HFs. Our results indicate that an n/c-MYC, NAMPT and SIRT1 connecting feedback loop may be active in both, the stem cell areas of the IFE and the HF, as well as in BCCs. NAMPT and SIRT1 were expressed together with n-MYC and c-MYC in HFs. In BCCs, only n-MYC, and in the stratum basale only c-MYC were co-expressed together with NAMPT and SIRT1. These findings point to a novel association of the oncogenic drivers Hh and n-MYC in BCC with the targetable enzymes NAMPT and SIRT1. These observations may open novel avenues for therapeutic intervention strategies in BCCs.

MATERIALS AND METHODS

Specimens

Formalin-fixed paraffin-embedded tissue from 65 human BCCs were enrolled in this study. The specimen were taken from the archives of the Department of Pathology, Ludwig-Maximilians University, Munich. The BCCs were classified according to the World Health Organization (WHO) Skin Tumor Classification 2003. Tumours with more than one growth pattern were classified according to the predominant component for the purpose of this study. Twenty-six normal human skin specimens were taken from Burow's triangles of adjacent skin of non-BCC lesions. Dorsal or ventral skin was obtained from wild-type C57BL/6 mice (*n* = 6). Mice were maintained in the animal facility at the Pathology Institute (Ludwig-Maximilians University, Munich) in individually ventilated cages. Animal procedures were carried out in compliance with the institutional guidelines of the Ludwig-Maximilians University and the local government (Government of Upper Bavaria).

Immunohistochemistry

Immunohistochemical (IHC) staining was carried out using 3-μm thick consecutive sections using standard IHC protocols (for details see **Table I**). All primary antibody incubations were done at room temperature for 1 h. Slides were counterstained with haematoxylin. System controls without primary antibodies, as well as immunoglobulin isotype control antibodies were included for confirmation of staining specificity.

Staining specificity for the NAMPT antibody was also validated using mouse tissue in which both *nampt* alleles had been deleted by Cre recombinase. For validation of NAMPT and SIRT1 antibody specificity, siRNA-knockdown was employed in human cell lines, followed by cell embedding in paraffin and IHC staining. Unless otherwise indicated, the same conditions were applied for human and mouse tissue.

Assessment of immunohistochemistry

Sections were examined by 2 histopathologists (TK and LB) using light microscopy. Human and mouse c-/n-MYC, SIRT1, and DBC1 proteins were evaluated regarding the number of cells positive for nuclear staining, and NAMPT was evaluated regarding the number of nuclear and/or cytoplasmic positive cells. For all proteins staining intensity was not taken into consideration. A scoring system for n-MYC, SIRT1, and DBC1 was introduced as followed: score 0 for 0% positive cells, score 1 for 1–30% positive cells, score 2 for 31–60% positive cells and score 3 for 61–100% positive cells. For c-MYC the following scoring system was introduced: score 0 for 0–15% positive cells, score 1 for 16–100% positive cells.

RESULTS

c-MYC, NAMPT, SIRT1, DBC1, n-MYC and Ki-67 expression in normal human and mouse interfollicular epidermis

Our analyses of 26 normal skin samples consistently revealed nuclear c-MYC expression in approximately

Table I. List of antibodies and immunohistochemistry protocols

| Antibody/ (cat. No.)	Company	1° Ab dilution tissue		Pre-treatment	Detection system		Chromogen
		Human	Murine				
n-MYC polyclonal rabbit (23960002)	Novus Biologicals, Cambridge, UK	1:200	1:200	Epitope Retrieval Solution pH6 Novocastra, Wetzlar, Germany, (Cat.No. RE7113)	ImmPress Reagent Kit Rabbit Ig, Vector Laboratories, (Cat.No. MP-7401)		DAB+, Agilent Technologies, (Cat.No. K3468)
c-MYC monoclonal rabbit (ab32072)	Abcam, Cambridge, UK	1:120	1:120	Target Unmasking Fluid Pan Path, Budel, Netherlands, (Cat.No. Z000R0000)	Human tissue Vectastain ABC-Kit Elite Universal Vector Laboratories, (Cat.No. PK-6200)	Murine tissue ImmPress Reagent Kit Rabbit Ig, Vector Laboratories, (Cat.No. MP-7401)	DAB+, Agilent Technologies, (Cat.No. K3468)
SIRT1 polyclonal rabbit (HPA006295)	Atlas Antibodies, Stockholm, Sweden	1:250	1:300	Target Retrieval Solution Citrate pH6, Agilent Technologies, (Cat.No. S2369)	ImmPress Reagent Kit Rabbit Ig, Vector Laboratories, (Cat.No. MP-7401)		AEC+, Agilent Technologies, (Cat.No. K3469)
NAMPT polyclonal rabbit (HPA047776)	Atlas Antibodies, Stockholm, Sweden	1:200	1:200	Pro Taqs II Antigen-Enhancer pH9,5 (Quartett, Cat. No. 401602192)	ImmPress Reagent Kit Rabbit Ig, Vector Laboratories, (Cat.No. MP-7401)		DAB+, Agilent Technologies (Cat.No. K3468)
DBC1 (KIAA1967) polyclonal rabbit (ab84384)	Abcam, Cambridge, UK	1:100	1:150	Target Retrieval Solution Citrate pH6, Agilent Technologies, (Cat.No. S2369)	ImmPress Reagent Kit Rabbit Ig, Vector Laboratories, (Cat.No. MP-7401)		DAB+, Agilent Technologies, (Cat.No. K3468)
Ki-67 (SP6) monoclonal rabbit (275R-15)	Cell Marque, California, USA	1:200	1:200	Target Retrieval Solution pH6, Agilent Technologies, (Cat. No 1699)	ImmPress Reagent Kit Rabbit Ig, Vector Laboratories, (Cat.No. MP-7401)		AEC+, Agilent Technologies, (Cat.No. K3469)
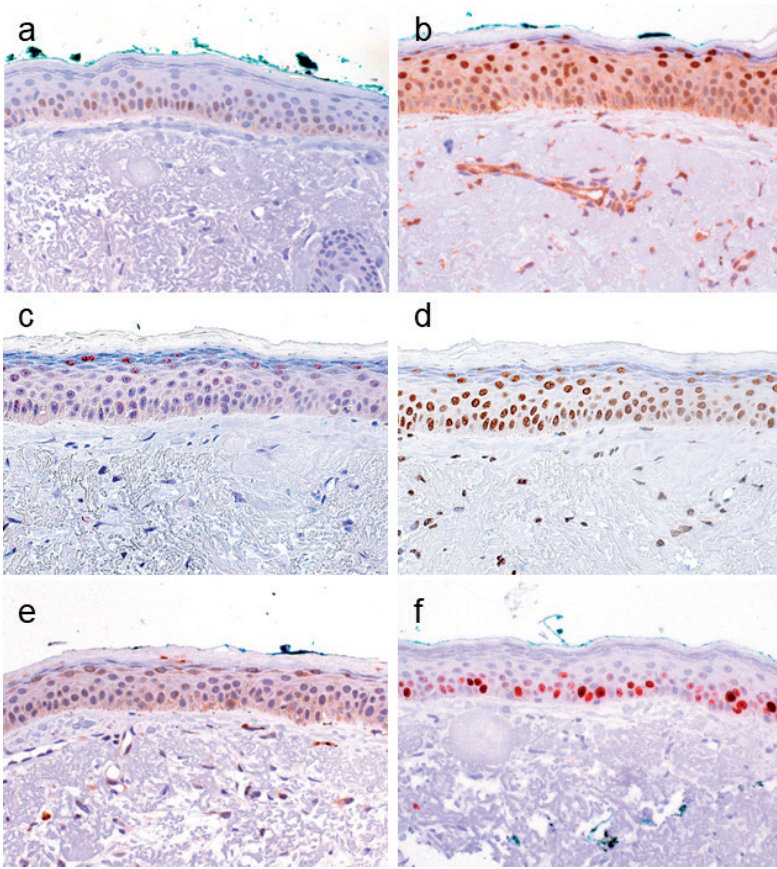
Fig. 1. c-MYC, NAMPT, SIRT1, DBC1, n-MYC and Ki-67 expression in normal human interfollicular epidermis. (a) Immunohistochemical analyses of normal human skin ($n = 26$) revealed that 20–60% of epidermal cells of the stratum basale, and 10–40% of cells in the stratum spinosum expressed c-MYC. (c) In both layers expression of SIRT1 was detected in 30–50% of cells. (b) NAMPT and (d) DBC1 were expressed in all cells of the stratum basale and stratum spinosum. In the latter nuclear NAMPT was more pronounced than cytoplasmic staining. SIRT1 expression was also detected in 20% of the cells of the stratum granulosum. (e) Positive n-MYC expression was detected in 10% of cells of the stratum basale and the stratum spinosum, and in 5% of cells in the stratum granulosum. (f) In the stratum basale 70–80% of cells stained positive for Ki-67. (Original magnification ×400).
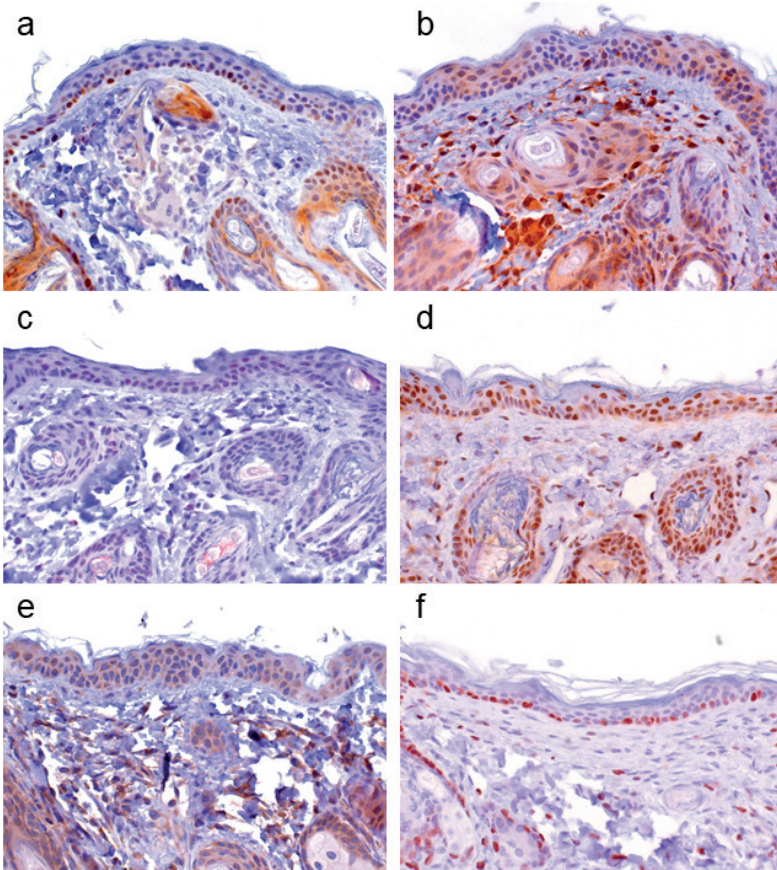

Fig. 2. c-MYC, NAMPT, SIRT1, DBC1, n-MYC and Ki-67 expression in normal murine interfollicular epidermis. (a) Immunohistochemical analyses of normal mouse skin ($n = 6$) revealed c-MYC expression in approximately 20–60% of the cells in the stratum basale, and in 10–40% of cells in the stratum spinosum. (b) NAMPT was expressed in all cells of the stratum basale and stratum spinosum. (c) SIRT1 was detected in the stratum basale in 60% of cells, in the stratum spinosum in 40% of cells, and in the stratum granulosum in 20% of cells. (d) In the stratum basale and stratum spinosum 80% cells were positive for DBC1. (e) n-MYC expression was found in 10% of cells of the stratum basale and the stratum spinosum. In the stratum granulosum 5% of cells expressed n-MYC. (f) Ki-67 positivity was observed in 80–100% of cells in the stratum basale. (Original magnification ×400).

20–60% of the cells in the stratum basale, and 10–40% of cells in the stratum spinosum (**Fig. 1**a). In the basal layer all cells expressed NAMPT and DBC1 (Fig. 1b, d). Also, the spinous layer was positive for both proteins, but NAMPT nuclear localization was more pronounced and cytoplasmic staining was reduced. Nuclear SIRT1 expression was detected in the cells of the stratum basale and stratum spinosum (each 30–50% positive cells), and in a few cells (20%) of the stratum granulosum (Fig. 1c). n-MYC expression was detected in the nucleus of a few cells of the stratum basale and stratum spinosum (each 10% positive cells). In the stratum granulosum 5% of the cells expressed n-MYC (Fig. 1e). Ki-67 staining was found to be positive in 70–80% of cells of the stratum basale (Fig. 1f). In murine skin we observed a similar expression pattern of the proteins (**Fig. 2**). Human and mouse IFE IHC expression data is summarized in **Table II**.

Taken together positivity for c-MYC in the two lower epidermal layers was associated with NAMPT and SIRT1 expression, suggesting that there may be a c-MYC-driven activation of the components of the feedback loop in the proliferative layers of the skin.

c-MYC, NAMPT, SIRT1, DBC1, n-MYC and Ki-67 expression in human and murine hair follicles

In order to determine whether common pathways are active in BCCs and in cells from which BCCs most likely derive (2, 3), we set out to determine the expression of c-MYC, NAMPT, SIRT1, DBC1, n-MYC and Ki-67 in normal human and mouse skin HF in anagen, and for the secondary hair germ in the telogen to anagen transition phase of the hair cycle.

In human HF, 60% of the infundibulum and 40–60% of the isthmus cells stained positive for c-MYC (**Fig. 3**a). In the bulge region 60% of cells were positive. No c-MYC staining was observed in the hair matrix and dermal papillae. c-MYC expression was lower in the inner root sheath (IRS) (5–20% positive cells), than in the outer root sheath (ORS) (20–60% positive cells). NAMPT, SIRT1 and DBC1 were expressed in the whole HF with 50–70% positive cells in the bulge region, and 50% positive cells in the HF matrix (Fig. 3b–d). They were expressed in 20–50% of cells in the lower ORS, overlapping with areas of high n-MYC expression (10–50%) (Fig. 3b–e). In the IRS more cells were positive for n-MYC (30–60%) (Fig. 3e). In the bulge region 60–80% of the cells were n-MYC

Table II. Percentage of cells expressing c-MYC, NAMPT, SIRT1, DBC1, n-MYC and Ki-67 in normal human and murine skin and in the anagen, or telogen and early anagen (secondary hair germs) phase of the hair cycle in human and murine hair follicles (HF)

| Protein	Human skin and HF (%)	Mouse skin and HF (%)	Protein	Human skin and HF (%)	Mouse skin and HF (%)
c-MYC			DBC1		
Stratum basale	20–60	20–60	Stratum basale	100	80
Stratum spinosum	10–40	10–40	Stratum spinosum	100	80
Infundibulum	60	80	Infundibulum	40	30
Isthmus	40–60	50	Isthmus	40–60	50–70
Bulge region	60	40–60	Bulge region	50–70	30
Hair matrix	0	0	Hair matrix	50	20
Dermal papillae	0	0	Dermal papillae	0	0
Outer root sheath	20–60	40–60	Outer root sheath	20–50	70
Inner root sheath	5–20	5	Inner root sheath	20–30	30
Secondary hair germ	40–60	50	Secondary hair germ	40	20–40
NAMPT			n-MYC		
Stratum basale	100	100	Stratum basale	10	10
Stratum spinosum	100	100	Stratum spinosum	10	10
Infundibulum	40	60	Stratum granulosum	5	5
Isthmus	40	30–40	Infundibulum	70	60
Bulge region	50–70	50	Isthmus	40–60	60
Hair matrix	50	30	Bulge region	60–80	60
Dermal papillae	0	0	Hair matrix	70–100	100
Outer root sheath	20–50	40–60	Dermal papillae	0	0
Inner root sheath	30–60	20–40	Outer root sheath	10–50	60–80
Secondary hair germ	50	40–60	Inner root sheath	30–60	40
SIRT1			Secondary hair germ	40–60	40
Stratum basale	30–50	60	Ki-67		
Stratum spinosum	30–50	40	Stratum basale	70–80	80–100
Stratum granulosum	20	20	Infundibulum	60	40–70
Infundibulum	60	40–60	Isthmus	30	10–30
Isthmus	40	30	Bulge region	20	40–70
Bulge region	50–70	50	Hair matrix	0	0
Hair matrix	50	30	Dermal papillae	0	0
Dermal papillae	0	0	Outer root sheath	40	70
Outer root sheath	20–50	60	Inner root sheath	5	5–30
Inner root sheath	20–50	20	Secondary hair germ	10–20	30–50
Secondary hair germ	40–60	40			
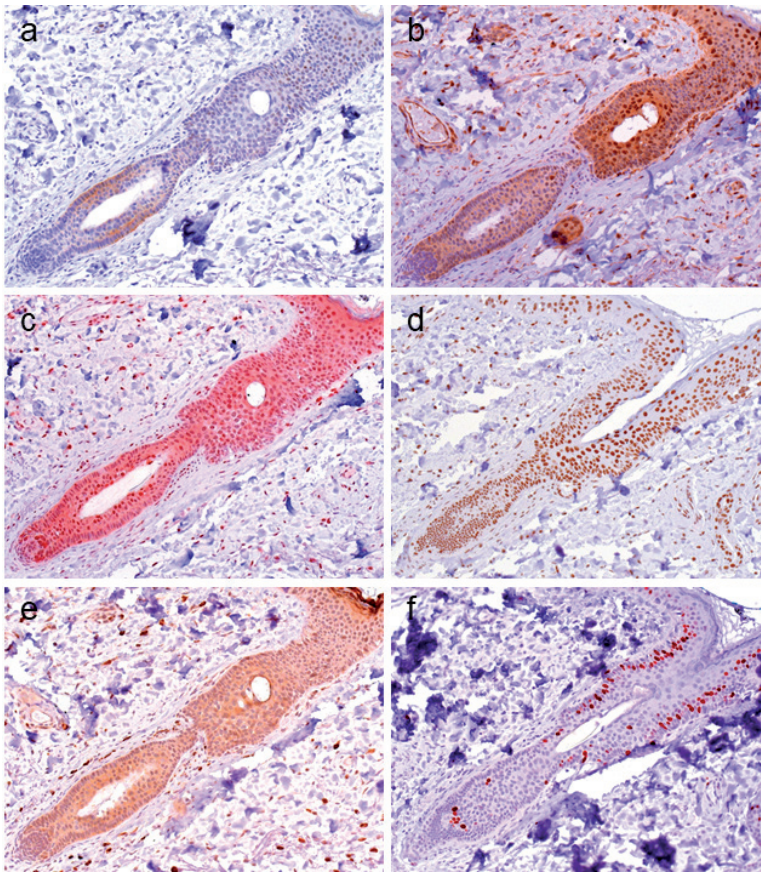
Fig. 3. c-MYC, NAMPT, SIRT1, DBC1, n-MYC and Ki-67 expression in normal human hair follicles. (a) In the hair follicle (HF) infundibulum 60% of cells, and in the isthmus 40–60% of the cells stain positive for c-MYC. In the bulge region 60% c-MYC positive cells were detected in the middle suprabulbar region, whereas regions above and underneath the central region in the suprabulbar region were negative. No c-MYC staining was observed in the hair matrix and dermal papillae. The expression of c-MYC was lower in the inner (5–20% positive cells) than in the outer root sheath (20–60% positive cells). (b) NAMPT, (c) SIRT1 and (d) DBC1 were detected in the whole HF with enhancement in the bulge region (50–70% positive cells) and follicular matrix (50% positive cells). (e) n-MYC staining was detected in the follicular outer (10–50% positive cells) and inner root sheath (30–60% positive cells), in the bulge region (60–80% positive cells) and the HF matrix (70–100% positive cells). (f) Ki-67 expressing cells were located in the infundibulum (60% positive cells), the isthmus (30% positive cells), the HF bulge (20% positive cells), the ORS (40% positive cells) and the IRS (5% positive cells). (Original magnification ×200).
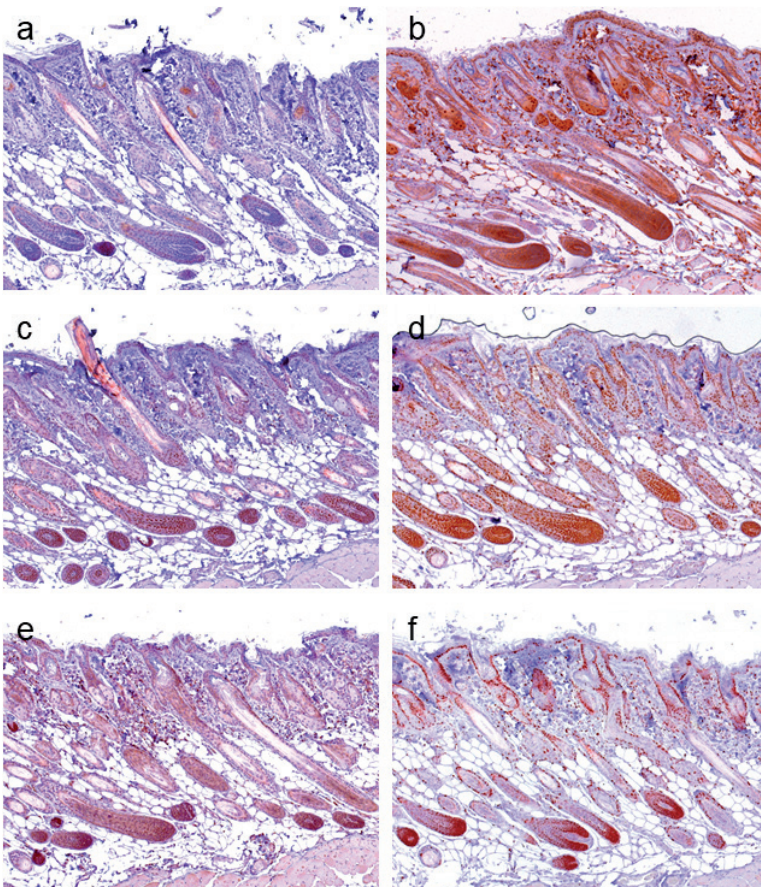

Fig. 4. c-MYC, NAMPT, SIRT1, DBC1, n-MYC and Ki-67 expression in murine hair follicles. (a) In the upper bulge region 40–60% of the cells expressed c-MYC, whereas regions in the lower and central bulge were negative. We found 80% c-MYC positive cells in the infundibulum and no c-MYC staining in the hair matrix and dermal papillae. The expression of c-MYC was lower in the inner, than in the outer root sheath (5% vs. 40–60% positive cells). (b) NAMPT was detected in 60% of cells of the infundibulum, 30–40% of cells of the isthmus, 50% of cells of the bulge region and 30% of cells in the hair matrix. In the dermal papillae NAMPT was not expressed. In the outer root sheath the expression of NAMPT was higher (40–60% positive cells) compared with the inner root sheath (20–40% positive cells). (c) SIRT1 was detected in the whole hair follicle (HF) except for the dermal papillae, with 40–60% positive cells in the infundibulum, 30% positive cells in the isthmus, 50% positive cells in the bulge region, 30% positive cells in the hair matrix, 60% positive cells in the outer root sheath, and 20% positive cells in the inner root sheath. (d) DBC1 was expressed in the whole HF except for the dermal papillae with enhancement in the isthmus (50–70% positive cells) and the outer root sheath (70% positive cells). (e) N-MYC staining was detected in the hair matrix (100% positive cells), infundibulum (60% positive cells), isthmus (60% positive cells), bulge region (60% positive cells), inner root sheath (40% positive cells) and outer root sheath (50% positive cells). (f) Ki-67 expressing cells were predominantly located in the infundibulum and bulge region (40–70% positive cells), in the isthmus (10–30% positive cells) and in the outer root sheath (70% positive cells). (Original magnification ×100).
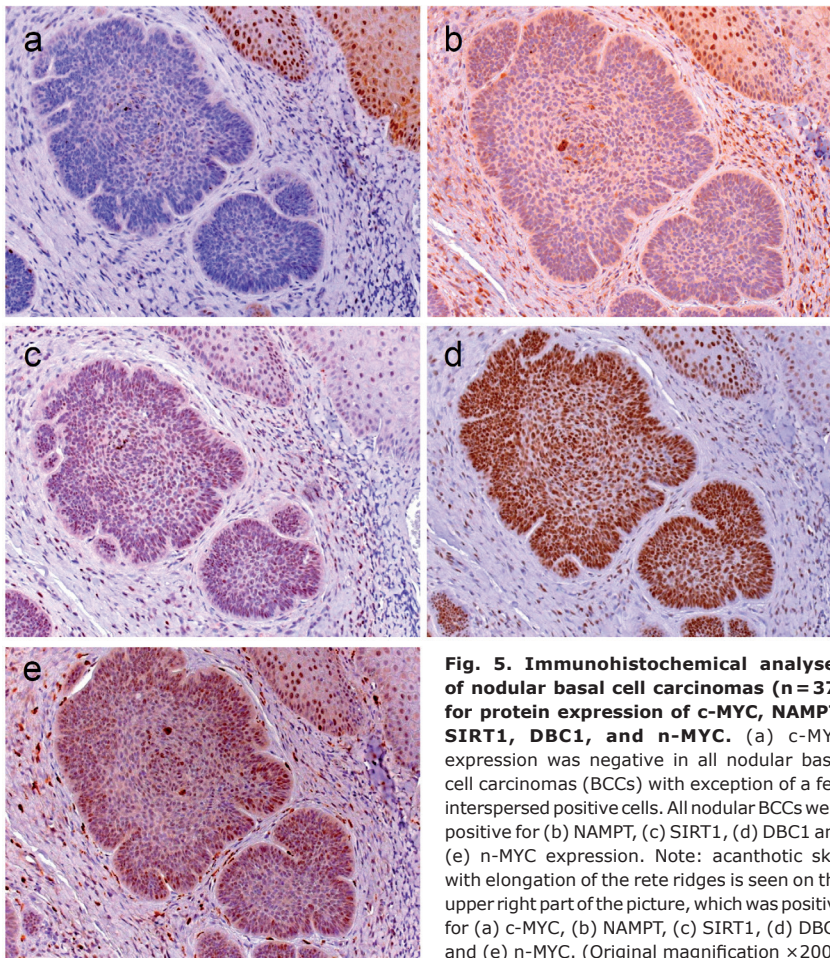
Fig. 5. Immunohistochemical analyses of nodular basal cell carcinomas (n = 37) for protein expression of c-MYC, NAMPT, SIRT1, DBC1, and n-MYC. (a) c-MYC expression was negative in all nodular basal cell carcinomas (BCCs) with exception of a few interspersed positive cells. All nodular BCCs were positive for (b) NAMPT, (c) SIRT1, (d) DBC1 and (e) n-MYC expression. Note: acanthotic skin with elongation of the rete ridges is seen on the upper right part of the picture, which was positive for (a) c-MYC, (b) NAMPT, (c) SIRT1, (d) DBC1 and (e) n-MYC. (Original magnification ×200).

of cells positive for Ki-67. The matrix was negative for Ki-67 staining. The mesenchymal dermal papillae was negative for all tested proteins (Fig. 3). In the secondary hair germ in human telogen phase HF, c-MYC, SIRT1 and n-MYC were expressed in 40–60% of cells, NAMPT in 50%, DBC1 in 40% and Ki-67 in 10–20% of the cells (data not shown). In the murine HF a similar distribution pattern of the proteins was detected (**Fig. 4**). Human and mouse HF expression data is summarized in Table II. Taken together, areas with the strongest n-MYC expression, such as the bulge region and hair matrix also displayed the highest NAMPT, SIRT1 and DBC1 expression. This distribution pattern was similar in human and mouse skin, suggesting a conserved functional connection and putative role for n-MYC, NAMPT, SIRT1 and DBC1 as a regulatory circuit in stem cells and transient amplifying cells of HF in mammals.

c-MYC, NAMPT, SIRT1, DBC1 and n-MYC expression in basal cell carcinoma

To determine whether a c-/n-MYC-NAMPT-SIRT1 positive feedback loop may be active in BCCs, we investigated a collection of 65 BCCs, comprising nodular (n = 37), micronodular (n = 4), superficial (n = 13), infiltrative (n = 8), and fibroepithelial (n = 3) subtypes. Irrespective of the morphological tumour subtype we did not detect c-MYC expression except for a few interspersed positive cells, as shown for nodular (**Fig. 5**a) and superficial BCCs (**Fig. 6**a) (score 0 in all cases). All BCC histological subtypes

positive. In the HF matrix most cells expressed n-MYC (70–100%). Inside the matrix the number of n-MYC positive cells gradually decreased with the differentiation from lower to upper layers. Sixty percent of the cells in the infundibulum and 30% of cells in the isthmus were Ki-67 positive (Fig. 3f). The expression of Ki-67 was weaker in the IRS (5% positive cells) than in the ORS (40% positive cells). The HF bulge region revealed 20%

Table III. Expression of c-MYC, NAMPT, SIRT1, DBC1 and n-MYC in different subtypes of basal cell carcinomas (BCCs)

| Protein	BCC total number of cases n (%)	Nodular n = 37 n (%)	Superficial n = 13 n (%)	Infiltrative n = 8 n (%)	Micronodular n = 4 n (%)	Fibroepithelial n = 3 n (%)
c-MYC						
Score 0	65/65 (100)	37/37 (100)	13/13 (100)	8/8 (100)	4/4 (100)	3/3 (100)
NAMPT						
Score 1	3/65 (5)	3/37 (8)	0	0	0	0
Score 2	10/65 (15)	6/37 (16)	2/13 (15)	1/8 (12)	1/4 (25)	0
Score 3	52/65 (80)	28/37 (76)	11/13 (85)	7/8 (88)	3/4 (75)	3/3 (100)
SIRT1						
Score 1	5/65 (8)	2/37 (5)	2/13 (15)	0	0	1/3 (33)
Score 2	9/65 (14)	5/37 (14)	1/13 (8)	2/8 (25)	1/4 (25)	0
Score 3	51/65 (78)	30/37 (81)	10/13 (77)	6/8 (75)	3/4 (75)	2/3 (67)
DBC1						
Score 3	65/65 (100)	37/37 (100)	13/13 (100)	8/8 (100)	4/4 (100)	3/3 (100)
n-MYC						
Score 1	22/65 (34)	10/37 (27)	6/13 (46)	3/8 (37)	2/4 (50)	1/3 (33)
Score 2	15/65 (23)	10/37 (27)	2/13 (15)	1/8 (13)	1/4 (25)	1/3 (33)
Score 3	28/65 (43)	17/37 (46)	5/13 (39)	4/8 (50)	1/4 (25)	1/3 (33)
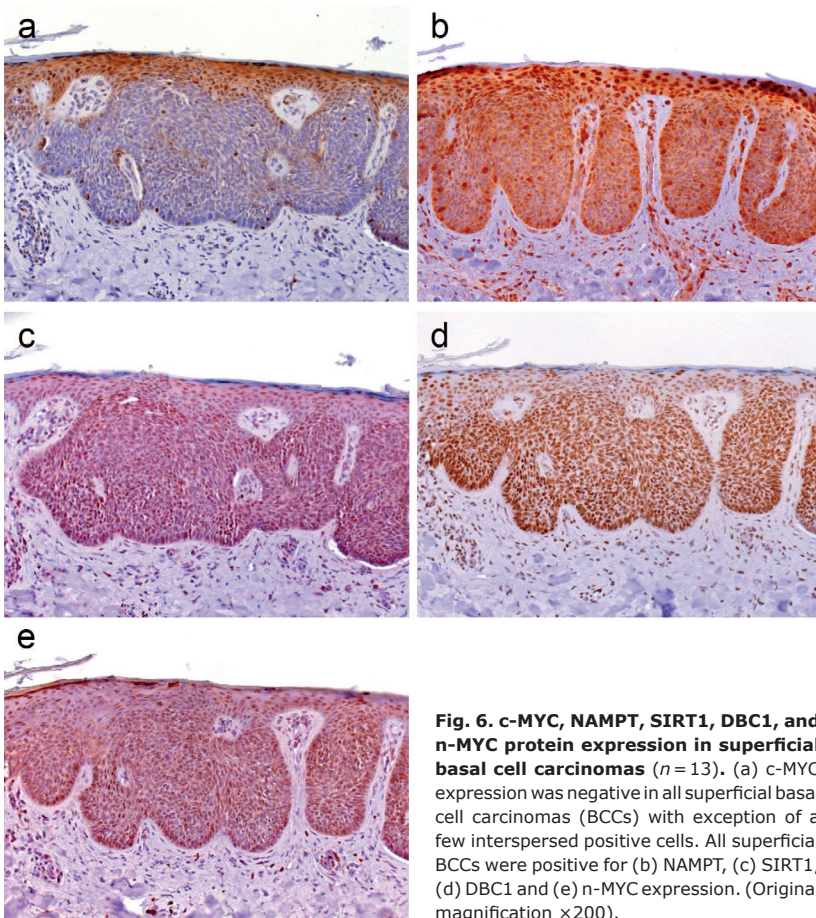
Fig. 6. **c-MYC, NAMPT, SIRT1, DBC1, and n-MYC protein expression in superficial basal cell carcinomas** ($n = 13$). (a) c-MYC expression was negative in all superficial basal cell carcinomas (BCCs) with exception of a few interspersed positive cells. All superficial BCCs were positive for (b) NAMPT, (c) SIRT1, (d) DBC1 and (e) n-MYC expression. (Original magnification ×200).

n-MYC is summarised in **Table III** and graphically depicted in **Fig. 7**. All BCC subtypes consistently had a score 0 expression pattern for c-MYC, and score 3 for DBC1. All were positive for n-MYC, NAMPT and SIRT1 expression with only slight differences in the number of score 1, score 2 and score 3 cases in the different histological BCC subtypes (Fig. 7). Taken together, positivity of all analysed cases indicate a potential involvement of n-MYC, NAMPT and SIRT1 in BCC pathogenesis in general, independent of the individual subtype.

DISCUSSION

Deregulated Hh signalling plays a crucial role in the tumorigenesis of BCCs. Various Hh pathway activation strategies targeting different stem cell populations have been employed to initiate BCCs in mice and have allowed identification of the cells of BCC origin. According to these studies BCCs arise from HF and IFE progenitor/stem cells; from stem cells in the bulge, secondary hair germ, the isthmus, and the mechanosensory touch dome epithelia (2, 3). In the putative cells of BCC origin that we were able

were positive for n-MYC, NAMPT, SIRT1 and DBC1. Results for nodular and superficial BCCs are shown in Fig. 5b–e and Fig. 6b–e. Almost all BCCs cells and the adjacent normal epithelial cells expressed DBC1 (Score 3 in 100% of BCCs) indicating that DBC1 was not differentially expressed. Detailed expression data for all BCC subtypes of c-MYC, NAMPT, SIRT1, DBC1 and

to identify, we detected the highest expression of NAMPT and SIRT1, in addition to high n-MYC and c-MYC levels, compared with other skin areas. This high expression pattern was most pronounced in the bulge region, and it was also present in the isthmus and the secondary hair germ. Since a similar expression pattern was present in murine skin, our data point to a putative evolutionary
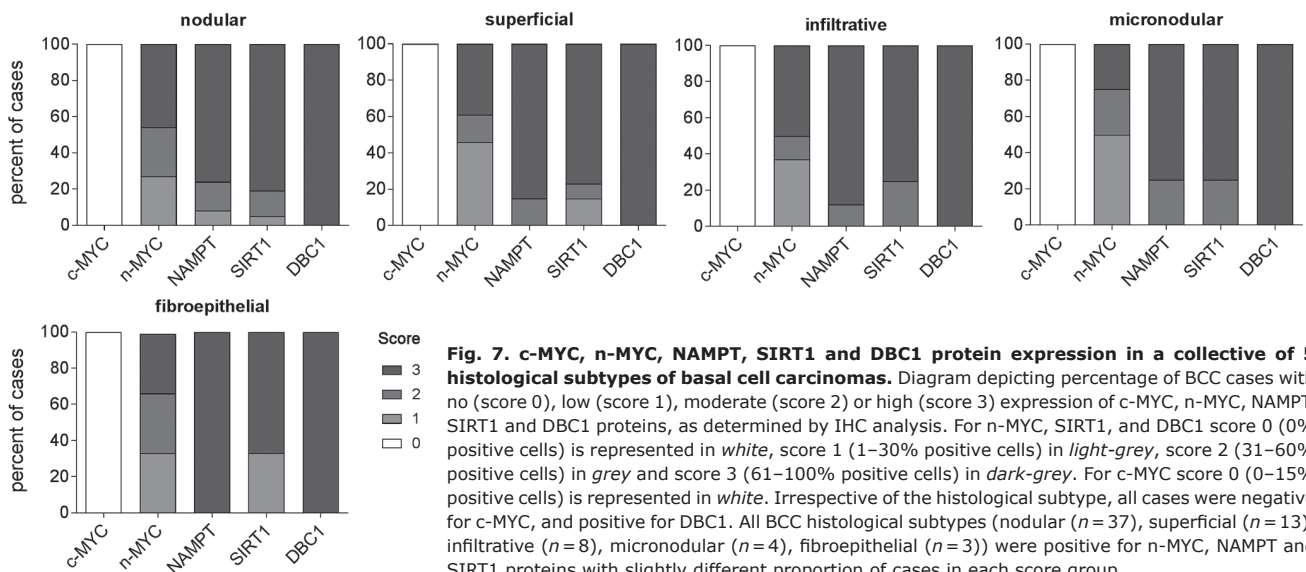

Fig. 7. **c-MYC, n-MYC, NAMPT, SIRT1 and DBC1 protein expression in a collective of 5 histological subtypes of basal cell carcinomas.** Diagram depicting percentage of BCC cases with no (score 0), low (score 1), moderate (score 2) or high (score 3) expression of c-MYC, n-MYC, NAMPT, SIRT1 and DBC1 proteins, as determined by IHC analysis. For n-MYC, SIRT1, and DBC1 score 0 (0% positive cells) is represented in *white*, score 1 (1–30% positive cells) in *light-grey*, score 2 (31–60% positive cells) in *grey* and score 3 (61–100% positive cells) in *dark-grey*. For c-MYC score 0 (0–15% positive cells) is represented in *white*. Irrespective of the histological subtype, all cases were negative for c-MYC, and positive for DBC1. All BCC histological subtypes (nodular ($n = 37$), superficial ($n = 13$), infiltrative ($n = 8$), micronodular ($n = 4$), fibroepithelial ($n = 3$)) were positive for n-MYC, NAMPT and SIRT1 proteins with slightly different proportion of cases in each score group.

conservation, and suggested a potential functional role of the factors of the positive feedback loop in skin stem cells.

In the lower ORS of the hair matrix c-MYC was not detected, but high n-MYC expression was observed, together with strong Ki-67 positivity. This region contains the fastest cycling cells that express high levels of the Hh effector Gli1 (6). Studies in mice have shown that n-Myc drives proliferation in this region of the hair matrix (6). In the bulb region of the hair matrix the cells are subjected to a layer specific differentiation programme as the cells move upwards to compose the mature HF epithelium. In agreement with down-regulation of c-MYC during terminal differentiation (20, 21), c-MYC was not expressed here. However, this region was characterised by high n-MYC, NAMPT and SIRT expression levels, indicating that the positive feedback loop factors may be involved in processes leading to differentiation of transit amplifying cells in the hair matrix.

The expression of epidermal n-Myc is differentially regulated during murine development from negative (6, 22) to weakly positive (23). In the fully differentiated epidermis of adult humans and mice we detected n-MYC expression in dispersed cells, which is in agreement with recent results demonstrating n-Myc expression in adult mouse epidermis by immunoblot analysis (24). Previous studies have shown that n-Myc is preferentially expressed in stem cells, which are in the earliest stage of differentiation (23, 25, 26). Therefore, the few n-MYC-positive cells we detected in the stratum basale may represent stem cells that are in the process of differentiation, probably belonging to one of the two recently identified heterogeneous populations of stem cells in the basal layer (27).

In the human IFE, c-MYC is required for proliferation of progenitors in the basal epidermal layer to replenish this layer, and give rise to non-proliferative suprabasal epidermal layers. According to Berta et al. (28) and Watt et al. (29) c-MYC may also induce differentiation in the IFE, representing a fail-safe mechanism to prevent uncontrolled proliferation of the stem cell compartment. While low levels of c-MYC may induce proliferation and stem cell expansion, high levels may trigger terminal differentiation (28). Our study revealed 20–60% c-MYC positive cells in the basal layer. It reflects the proliferative heterogeneity of this layer of human IFE (30) and was accompanied by Ki-67 positivity. As cytoplasmic NAMPT and nuclear SIRT1 expression was found in the basal layer of IFE in addition to c-MYC, this may indicate that both proteins might be downstream effectors of c-MYC contributing to maintenance and self-renewal of stem cells in this layer, corresponding to a previously reported role of NAMPT and SIRT1 in other stem cells (reviewed in (31, 32)).

In addition, c-MYC was expressed, although at a lower level than in the basal layer, in dispersed cells in the stratum spinosum. Interestingly, in this layer the NAMPT subcellular localization was more nuclear, which has been associated with differentiation and cell cycle arrest (33, 34), and which is consistent with the commitment of cells to a programme of terminal differentiation in this skin layer.

High n-MYC protein expression in all types of BCCs confirmed previous findings (35, 36). Various alterations contribute to deregulation of n-MYC in BCCs, such as copy-gain of the *MYCN* locus, missense mutations disabling proteasomal degradation, or by induction through Hh signalling (4, 35). Throughout our BCC collection we exclusively detected n-MYC, and absence of c-MYC expression. As demonstrated in *MYCN*-amplified neuroblastomas, negative cross regulation by n-MYC can lead to down-regulation of c-MYC (37). Therefore, MYC family member autoregulation may lead to repression of c-MYC in BCCs.

Together with n-MYC, we observed high NAMPT and SIRT1 protein expression in BCCs. Interestingly, n-MYC and SIRT1 are connected through a positive feedback regulation in neuroblastomas (38). Accordingly, our data may indicate that NAMPT, and the NAD$^+$-dependent SIRT1 protein deacetylase are likely to be downstream of n-MYC and linked in a positive feedback loop in BCCs. Since we also observed the expression of these proteins in the putative cells of BCCs origin, this continuity of expression pattern in stem cells and BCCs points to a potential involvement of the oncogenic MYC-NAMPT-SIRT1 signalling pathway in development of BCCs. Experimental models have revealed that the tumour histological phenotype can reflect the cellular origin, e.g. mouse tumours originating from hair follicles appear nodular, and those derived from IFE resemble superficial human BCCs (2). Our collection showed slight differences concerning the percentage of positive cells in individual cases, leading to small differences in the proportion of score 1, score 2 and score 3 cases in the different histological subtypes. However, as the number of cases of various subtypes was small in our collection further investigations will be necessary to confirm these differences and to investigate if there is a biological significance reflected by our scoring system.

Often, recurrent surgical approaches to locally advanced BCCs are not feasible (39). Moreover, patients develop resistance to therapeutic inhibitors, such as Vismodegib. To overcome resistance, combination therapies or strategies targeting downstream of SMO have been proposed (40). According to our results, NAMPT and SIRT1 may represent such targets. Increasing evidence indicates that targeting SIRT1 may be effective to eliminate cancer stem cells, and overcome drug resistance. In a recent phase III clinical trial the SIRT1 inhibitor nicotinamide significantly reduced the formation of new non-melanoma skin cancers (41). In addition, a lot of cancer cell types were shown to be sensitive to NAMPT inhibitors, leading, for instance, to chemosensitization of *MYCN*-amplified neuroblastomas. Therefore, inhibition of SIRT1 and/ or NAMPT, alone or in combination with conventional therapeutics, or as an adjuvant combination treatment may represent therapeutic strategies for targeting advanced, recurrent, therapy-resistant BCCs.

ACKNOWLEDGEMENTS

REFERENCES

1. Pellegrini C, Maturo MG, Di Nardo L, Ciciarelli V, Gutierrez Garcia-Rodrigo C, Fargnoli MC. Understanding the molecular genetics of basal cell carcinoma. Int J Mol Sci 2017; 18. pii: E2485.
2. Grachtchouk M, Pero J, Yang SH, Ermilov AN, Michael LE, Wang A, et al. Basal cell carcinomas in mice arise from hair follicle stem cells and multiple epithelial progenitor populations. J Clin Invest 2011; 121: 1768–1781.
3. Peterson SC, Eberl M, Vagnozzi AN, Belkadi A, Veniaminova NA, Verhaegen ME, et al. Basal cell carcinoma preferentially arises from stem cells within hair follicle and mechanosensory niches. Cell Stem Cell 2015; 16: 400–412.
4. Hatton BA, Knoepfler PS, Kenney AM, Rowitch DH, de Alboran IM, Olson JM, et al. N-myc is an essential downstream effector of Shh signaling during both normal and neoplastic cerebellar growth. Cancer Res 2006; 66: 8655–8661.
5. Kenney AM, Cole MD, Rowitch DH. Nmyc upregulation by sonic hedgehog signaling promotes proliferation in developing cerebellar granule neuron precursors. Development 2003; 130: 15–28.
6. Mill P, Mo R, Hu MC, Dagnino L, Rosenblum ND, Hui CC. Shh controls epithelial proliferation via independent pathways that converge on N-Myc. Dev Cell 2005; 9: 293–303.
7. Oliver TG, Grasfeder LL, Carroll AL, Kaiser C, Gillingham CL, Lin SM, et al. Transcriptional profiling of the Sonic hedgehog response: a critical role for N-myc in proliferation of neuronal precursors. Proc Natl Acad Sci U S A 2003; 100: 7331–7336.
8. Mullor JL, Dahmane N, Sun T, Ruiz i Altaba A. Wnt signals are targets and mediators of Gli function. Curr Biol 2001; 11: 769–773.
9. Kriegl L, Horst D, Kirchner T, Jung A. LEF-1 expression in basal cell carcinomas. Br J Dermatol 2009; 160: 1353–1356.
10. Saldanha G, Ghura V, Potter L, Fletcher A. Nuclear beta-catenin in basal cell carcinoma correlates with increased proliferation. Br J Dermatol 2004; 151: 157–164.
11. Boon K, Caron HN, van Asperen R, Valentijn L, Hermus MC, van Sluis P, et al. N-myc enhances the expression of a large set of genes functioning in ribosome biogenesis and protein synthesis. EMBO J 2001; 20: 1383–1393.
12. Malynn BA, de Alboran IM, O'Hagan RC, Bronson R, Davidson L, DePinho RA, et al. N-myc can functionally replace c-myc in murine development, cellular growth, and differentiation. Genes Dev 2000; 14: 1390–1399.
13. Dang CV. MYC on the path to cancer. Cell 2012; 149: 22–35.
14. Menssen A, Hermeking H. c-MYC and SIRT1 locked in a vicious cycle. Oncotarget 2012; 3: 112–113.
15. Menssen A, Hydbring P, Kapelle K, Vervoorts J, Diebold J, Luscher B, et al. The c-MYC oncoprotein, the NAMPT enzyme, the SIRT1-inhibitor DBC1, and the SIRT1 deacetylase form a positive feedback loop. Proc Natl Acad Sci U S A 2012; 109: E187–196.
16. Chalkiadaki A, Guarente L. The multifaceted functions of sirtuins in cancer. Nat Rev Cancer 2015; 15: 608–624.
17. Roth M, Chen WY. Sorting out functions of sirtuins in cancer. Oncogene 2014; 33: 1609–1620.
18. Wang Z, Chen W. Emerging Roles of SIRT1 in Cancer Drug Resistance. Genes Cancer 2013; 4: 82–90.
19. Kriegl L, Vieth M, Kirchner T, Menssen A. Up-regulation of c-MYC and SIRT1 expression correlates with malignant transformation in the serrated route to colorectal cancer.

20. Conacci-Sorrell M, McFerrin L, Eisenman RN. An overview of MYC and its interactome. Cold Spring Harb Perspect Med 2014; 4: a014357.
21. Dotto GP, Gilman MZ, Maruyama M, Weinberg RA. c-myc and c-fos expression in differentiating mouse primary keratinocytes. EMBO J 1986; 5: 2853–2857.
22. Hurlin PJ, Queva C, Koskinen PJ, Steingrimsson E, Ayer DE, Copeland NG, et al. Mad3 and Mad4: novel Max-interacting transcriptional repressors that suppress c-myc dependent transformation and are expressed during neural and epidermal differentiation. EMBO J 1995; 14: 5646–5659.
23. Mugrauer G, Alt FW, Ekblom P. N-myc proto-oncogene expression during organogenesis in the developing mouse as revealed by in situ hybridization. J Cell Biol 1988; 107: 1325–1335.
24. Flores A, Schell J, Krall AS, Jelinek D, Miranda M, Grigorian M, et al. Lactate dehydrogenase activity drives hair follicle stem cell activation. Nat Cell Biol 2017; 19: 1017–1026.
25. Thiele CJ, Reynolds CP, Israel MA. Decreased expression of N-myc precedes retinoic acid-induced morphological differentiation of human neuroblastoma. Nature 1985; 313: 404–406.
26. Zimmerman KA, Yancopoulos GD, Collum RG, Smith RK, Kohl NE, Denis KA, et al. Differential expression of myc family genes during murine development. Nature 1986; 319: 780–783.
27. Tan DW, Jensen KB, Trotter MW, Connelly JT, Broad S, Watt FM. Single-cell gene expression profiling reveals functional heterogeneity of undifferentiated human epidermal cells. Development 2013; 140: 1433–1444.
28. Berta MA, Baker CM, Cottle DL, Watt FM. Dose and context dependent effects of Myc on epidermal stem cell proliferation and differentiation. EMBO Mol Med 2010; 2: 16–25.
29. Watt FM, Frye M, Benitah SA. MYC in mammalian epidermis: how can an oncogene stimulate differentiation? Nat Rev Cancer 2008; 8: 234–242.
30. Jones PH, Simons BD, Watt FM. Sic transit gloria: farewell to the epidermal transit amplifying cell? Cell Stem Cell 2007; 1: 371–381.
31. Calvanese V, Fraga MF. SirT1 brings stemness closer to cancer and aging. Aging 2011; 3: 162–167.
32. Ahlqvist KJ, Suomalainen A, Hamalainen RH. Stem cells, mitochondria and aging. Biochim Biophys Acta 2015; 1847: 1380–1386.
33. Kitani T, Okuno S, Fujisawa H. Growth phase-dependent changes in the subcellular localization of pre-B-cell colony-enhancing factor. FEBS Lett 2003; 544: 74–78.
34. Romacho T, Villalobos LA, Cercas E, Carraro R, Sánchez-Ferrer CF, Peiró C. Visfatin as a Novel Mediator Released by Inflamed Human Endothelial Cells. PLoS One 2013; 8: e78283.
35. Bonilla X, Parmentier L, King B, Bezrukov F, Kaya G, Zoete V, et al. Genomic analysis identifies new drivers and progression pathways in skin basal cell carcinoma. Nat Genet 2016; 48: 398–406.
36. Freier K, Flechtenmacher C, Devens F, Hartschuh W, Hofele C, Lichter P, et al. Recurrent NMYC copy number gain and high protein expression in basal cell carcinoma. Oncology Reports 2006; 15: 1141–1145.
37. Breit S, Schwab M. Suppression of MYC by high expression of NMYC in human neuroblastoma cells. J Neurosci Res 1989; 24: 21–28.
38. Marshall GM, Liu PY, Gherardi S, Scarlett CJ, Bedalov A, Xu N, et al. SIRT1 Promotes N-Myc Oncogenesis through a Positive Feedback Loop Involving the Effects of MKP3 and ERK on N-Myc Protein Stability. PLoS Genet 2011; 7: e1002135.
39. Leffell DJ, Headington JT, Wong DS, Swanson NA. Aggressive-growth basal cell carcinoma in young adults. Arch Dermatol 1991; 127: 1663–1667.
40. Ridky TW, Cotsarelis G. Vismodegib resistance in basal cell carcinoma: not a smooth fit. Cancer Cell 2015; 27: 315–316.
41. Chen AC, Martin AJ, Choy B, Fernandez-Penas P, Dalziell RA, McKenzie CA, et al. A Phase 3 Randomized Trial of Nicotinamide for Skin-Cancer Chemoprevention. N Engl J Med 2015; 373: 1618–1626.